Development of Transgenic *Daphnia Magna* for Visualizing Homology-Directed Repair of DNA

Rizky Mutiara Fatimah
Osaka University
Nikko Adhitama
Osaka University
Yasuhiko Kato
Osaka University
Hajime Watanabe (watanabe@bio.eng.osaka-u.ac.jp)
Osaka University

Research Article

Keywords: transgenic, homology, DNA, HDR

Posted Date: September 22nd, 2021

DOI: https://doi.org/10.21203/rs.3.rs-888135/v1

Abstract

In the crustacean *Daphnia magna*, studying homology-directed repair (HDR) is important to understand genome maintenance during parthenogenesis, effects of environmental toxicants on the genome, and improvement of HDR-mediated genome editing. Here we developed a transgenic *D. magna* that expresses green fluorescence protein (GFP) upon HDR occurrence. We utilized the previously established reporter plasmid named DR-GFP that has a mutated *eGFP* gene (*SceGFP*) and the tandemly located donor *GFP* gene fragment (*iGFP*). Upon double-strand break (DSB) introduction on *SceGFP*, the *iGFP* gene fragment acts as the HDR template and restores functional eGFP expression. We customized this reporter plasmid to allow bicistronic expression of the *mCherry* gene under the control of the *D. magna EF1α-1* promoter/enhancer. By CRISPR/Cas-mediated knock-in of this plasmid via non-homologous joining, we generated the transgenic *D. magna* that expresses mCherry ubiquitously, suggesting that the DR-GFP reporter gene is expressed in most cells. Introducing DSB on the *SceGFP* resulted in eGFP expression and this HDR event could be detected by fluorescence, genomic PCR, and quantitative reverse-transcription PCR, suggesting this line could be used for evaluating HDR. The established reporter line might expand our understanding of the HDR mechanism and also improve the HDR-based gene-editing system in this species.

Introduction

Genomes are threatened by endogenously generated chemicals like reactive oxygen species and exogenous compounds such as mutagenic agents and radiation[1], which can lead to DNA double-strand breaks (DSBs). To ensure genetic stability and cellular viability, repairing the DSBs is essential. The DNA repair mainly occurs through non-homologous end joining (NHEJ) and homology-directed repair (HDR)[2]. The NHEJ leads to ligation of the two ends of the DNA strand during which insertion or deletion of nucleotides can often occur at the cleavage site. The HDR repairs the DSBs by using information copied from undamaged DNA that has an identical or homologous sequence (homology)[3] This homology-directed repair system can be divided into four sub-pathways based on the mechanistic difference: double-strand break repair (DSBR), synthesis-dependent strand annealing (SDSA), break-induced replication (BIR), and single-strand annealing (SSA)[2]. First, in the DSBR, the formation of an intermediate structure with holiday junctions (HJs) leads to the generation of crossover and non-crossover products[4]. Second, the SDSA exclusively generates the non-crossover products due to the lack of formation of the HJ structure[5]. Third, when only one ended DSB site has a sequence similar to that of the template, BIR occurs for non-reciprocal translocation of genetic information from template strand[6]. Fourth, when the DSB is induced between the tandem repeats of the highly homologous regions, the SSA repairs the DNA by pairing the homologous region followed by deletion of unpaired DNA and the intervening region[7]. In the mitotically proliferating cells, the SDSA is known to be the most common among the HDR sub-pathways[8].

The HDR also plays an important role in the field of genome editing. Following DSB using the programmable nuclease such as TALEN or CRISPR-Cas, a precise genome modification such as the codon replacements or the seamless integration of the fluorescent reporter gene is achieved via HDR with a donor DNA such as a plasmid or single-stranded oligo DNA (ssODN) flanked with right and left locus-specific homology arms[9,10]. However, the HDR efficiency reported in mammals and plants is lower compared to NHEJ[11,12,13] because it takes a longer time to complete than NHEJ[11] and functions only during S and G2 phases when the sister chromatid, the main template to repair DSB, is present[14]. Currently, several approaches have been developed to enhance genome editing by HDR such as inhibiting[15] or knocking out the key factor of NHEJ[16], synchronizing and capturing cells at the S and G2 phases[17], and modifying the Cas9 by fusing it with a key protein necessary in the HDR steps[18]. To evaluate the effects of these approaches on the HDR activity, the reporter system for visualizing the HDR event has been used[19].

Fluorescence live imaging of the HDR event is essential not only for investigating how and where the genome integrity is maintained in living organisms but also for evaluating the HDR activity by manipulating the components for DNA repair. The direct repeat GFP (DR-GFP) reporter assay has been established for fluorescence-based visualization of the HDR activity[20]. The DR-GFP reporter system is composed of two mutated eGFP genes. The upstream eGFP gene named *SceGFP* contains a recognition site of the rare-cutting I-SceI restriction enzyme. This recognition site contains two in-frame stop codons to terminate the protein expression. At downstream of the *SceGFP*, there is another mutated *eGFP* fragment termed internal GFP or *iGFP* that is an 812-bp internal GFP fragment. The HDR event can be detected by introducing a double-strand break (DSB) with I-SceI in the inactive *SceGFP* gene. The cleavage site will be repaired by HDR using *iGFP* as the template. Among the HDR sub-pathways, this DR-GFP system can visualize the non-crossover events that are mediated by the DSBR and SDSA[21], suggesting that this reporter can visualize the major HDR events spatiotemporally *in vivo*. This reporter has been applied to study the factors that contribute to HDR in mouse[22] and to study the role of a transcriptional repressor protein in HDR using *C. elegans* models[23].

The water flea *Daphnia magna* is a small freshwater crustacean found in broad continents such as Europe, Middle East, Central Asia, Africa, and North America[24]. The genus *Daphnia* reproduces by parthenogenesis under favorable environmental conditions but switches it to sexual reproduction in response to environmental stimuli such as shortened photoperiod, a lack of food, and/or increased population density[25]. To avoid the accumulation of deleterious mutations during the parthenogenetic cycle, *Daphnia* may have a unique HDR mechanism[26]. *D. magna* occupies an important position in the freshwater food chain and is highly sensitive to chemicals, which makes this species a model in environmental and toxicological studies. Thus, the effects of genotoxicants have been investigated at phenotypic level[27,28]. To understand their actions at the molecular level, it is important to study the DNA repair mechanism in this species. In the field of genome editing, the HDR-based knock-in of the exogenous DNA fragments has been reported in *D. magna*[16] as well as NHEJ-mediated knock-in [29,30]. The

HDR-based knock-in efficiency was low probably due to competition with the NHEJ pathway. To test this hypothesis, disruption *DNA ligase IV* that is the conserved component of the NHEJ pathway has been attempted[16]. However, its effect was not fully evaluated due to the lack of a method for quantifying the HDR event *in vivo*. Here we reported the development of an HDR reporter transgenic *Daphnia* by integrating the DR-GFP reporter system in *D. magna* genome. We confirm its functionality by introducing DSBs at the *SceGFP* region with the CRISPR/Cas9 system and could observe the HDR event with the eGFP signal spatiotemporally. Furthermore, by using this transgenic *Daphnia*, we could detect the repaired eGFP gene by genomic PCR and qPCR, which adds merit to this system to be utilized for the evaluation of the HDR event.

Materials And Methods

D. magna strain and culture condition

Wild type *D. magna* (NIES clone) was obtained from the National Institute of Environmental Studies (NIES, Tsukuba, Japan) and has been maintained in the laboratory for many generations. The *D. magna* was cultured under the following conditions: 80 juveniles (less than 24 h old) were collected and cultured in 5 L Artificial *Daphnia* Medium (ADaM)[31] at temperature 22-24^{o}C, under 16 h/8 h of light/dark photoperiod. *D. magna* were fed daily with 8 x 10^9 cells of *Chlorella vulgaris* (Oita Medaka Biyori, Oita, Japan) and 3 mg of baker's yeast (Marusan Pantry, Ehime, Japan) during the first week. Later, juveniles were removed daily and amounts of chlorella and yeast extract were doubled. The culture medium was changed once a week.

Generation of donor plasmid

To construct donor plasmid pEF1α-1::mCherry-2A-DR-GFP, chicken *β-actin* promoter of pDRGFP from Addgene No.26475[20] was replaced with *D. magna EF1α-1* promoter for ubiquitous expression. The fragment containing a complete sequence of *EF1α-1* promoter was derived from the previously constructed plasmid[29]. The two mutated eGFP fragments (*SceGFP* and *iGFP*) were amplified from the pDRGFP[20]. In the *SceGFP* region, a recognition site of TaqI, a four bases restriction enzyme, was introduced at two base pairs downstream of the I-SceI target site by substitution of two nucleotides. The TaqI recognition site will serve as a genome-wide DSB marker. Lastly, for the integration into *D. magna* genome, a 200 bp sequence of *scarlet* gene harboring a gRNA target sequence[32,33] was added. All assemblies were performed using GeneArt Cloning & Assembly (Invitrogen, Carlsbad, USA). The constructed donor plasmid was purified using FastGene Plasmid Mini Kit (Nippon Genetics, Tokyo, Japan) and sequenced. The donor plasmid used for microinjection was purified using PureYield Miniprep (Promega, Madison, USA) followed by phenol-chloroform purification, two times ethanol washing, and was re-suspended with ultrapure water (Invitrogen).

In vitro RNA synthesis

Guide RNAs (gRNAs) were synthesized using a cloning-free method from PCR-amplified template DNA as previously described[33]. The sense synthetic oligonucleotide containing a T7 promoter sequence, a gene-specific target sequence, and the first 20 nt of the Cas9 binding scaffold are shown in Table 1. gRNAs were synthesized using the MegaScript T7 Transcription Kit (Invitrogen), purified using Roche Mini Quick Spin RNA Column (Roche, Mannheim, Germany) followed by phenol/chloroform extraction, ethanol precipitation.

Table 1

The sense sequence of the oligonucleotide for guide RNA synthesis. A T7 promoter, a targeting sequence, and the first 20 bp of the Cas9 binding scaffold sequence were indicated with bold letters, underline, and italic letters respectively.

No	gRNA Target	Sense oligonucleotide
1	Scarlet (st)	5'-**GAAATTAATACGACTCACTATA** GGTTCACTCGTCGCCTTAAT*GTTTTAGAGCTAGAAA*-3'
2	Distal-less (Dll)	5'-**GAAATTAATACGACTCACTATA** GCAAGAAGATGCGCAAACCG*GTTTTAGAGCTAGAA*-3'
3	Scel	5'-**GAAATTAATACGACTCACTATA** GGTGTCGAGCTAGGGATAAC*GTTTTAGAGCTAGAA*-3'

For Cas9 mRNA synthesis, a template DNA containing T7 promoter sequence was PCR amplified from pCS-Dmavas-Cas9[34]. Capped mRNA synthesis and poly(A) tail addition were performed using mMessage mMachine T7 kit and Poly(A) Tailing Kit (Invitrogen) respectively. Synthesized mRNA was column purified, followed by phenol/chloroform extraction and ethanol precipitation. mRNA integrity and the addition of poly(A) tails were confirmed by denaturing formaldehyde gel electrophoresis.

Microinjection

Microinjection was performed following an established protocol[35,29]. In brief, the freshly ovulated *D. magna* eggs were collected from adult *D. magna* and placed in an ice-chilled M4 medium containing 80 mM sucrose (M4-sucrose). The injection solution was mixed with 2 mM Lucifer Yellow (Invitrogen) or 0.01 mM Alexa Fluor 568 Hydrazide (Invitrogen) for visualizing the volume of the injected solution. For the generation of the DR-GFP line, 1 μM Cas9 protein and 2 μM *scarlet* targeting gRNA (St gRNA) were used Before the Cas9 protein injection, Cas9 protein and gRNA were incubated at 37 ^{o}C for 5 minutes to form a ribonucleoprotein (RNP) complex. Microinjection was performed within two hours after the preparation of the solution. After injection, the intact eggs were transferred and cultured individually in a sterile 96 well plate filled with 100 μL of M4-sucrose and cultured in an incubator at 22^{o}C with 16 h/8 h of light/dark photoperiod for 3 days.

Phenotyping of the second antennae in embryos injected with distal-less (Dll) gRNA and Cas9

After co-injecting the Dll gRNA with Cas9 protein or mRNA, the degree of truncation of the second antennae was categorized following the previous study[35]. eGFP mRNA was co-injected with the Cas9 mRNA and Dll gRNA for confirmation of the mRNA integrity based on the eGFP fluorescence intensity. In normal phenotype, second antennae consist of a protopodite (*P*), carrying a dorsal and ventral ramus. Each ramus has three segments, Terminal (*T*), Middle (*M*), and Basal (*B*). There is an additional small wedge-shaped segment (*w*) between *B* and *P*. Mild truncation exhibit, a part of *M* and full *B* (ventral ramus), full *M*, *B*, and *w* (dorsal ramus). Medium truncation: a trace of *B* (ventral), *B* and *w* (dorsal). Strong truncation: only a trace of *B* and *w* (dorsal)[35].

Genotyping

Daphniids were collected and homogenized in 500 µL lysis buffer (50 mM Tris-HCl pH 7.5, 20 mM EDTA pH 8.0, 100 mM NaCl, 1% SDS) using MicroSmash homogenizer (TOMY, Tokyo, Japan) at 3000 rpm for 1.5 min with the presence of 0.15 mg/mL Proteinase K (Nacalai Tesque, Kyoto, Japan). The homogenized *daphniids* (lysate) were shaken overnight at 55^{o}C, 450 rpm using an incubator shaker (Bioshaker M-BR-022UP, TAITEC, Tokyo, Japan). To obtain genomic DNA (gDNA), the lysate was purified using phenol/chloroform extraction, precipitated with isopropanol, rinsed twice with 70% ethanol, and dissolved in 50 µL TE buffer before being used as a template for genomic PCR. The PCR was performed by using an Ex Taq Hot-Start DNA polymerase (TaKaRa) with primer sets amplifying the target region as described in Table 2.

Table 2

List of primers. The primers were synthesized by FASMAC (Tokyo, Japan).

Purpose	Target region	Direction	Sequence
Genotyping	mCherry	Forward	5'-GGCCATCATCAAGGAGTTC-3'
		Reverse	5'-CGTTGTGGGAGGTGATGTC-3'
	5' junction region of integration site	Forward	5'-TGGAGACGTCATTCGATTACG-3'
		Reverse	5'-CTGGCGTAATAGCGAAGAGG-3'
	3' junction region of integration site	Forward	5'-CAGCCATACCACATTTGTAG-3'
		Reverse	5'- GTTGAGCGACTGGTATCTTC – 3'
	Repaired eGFP	Forward	5'-CCAGACCGCCAAGCTG AAGGTGACC-3'
		Reverse	5'-ATCGCCCTCGCCCTCGCCG-3'
qPCR	Repaired eGFP	Forward	5'-TTCTAACATGCGGGGACGTG-3'
		Reverse	5'-CAGCTTGCCGTAGGTGGCAT-3'
	mCherry	Forward	5'-CTACGACGCTGAGGTCAAGAC-3'
		Reverse	5'-GGTGTAGTCCTCGTTGTGGG-3'
	L32	Forward	5'-GACCAAAGGGTATTGACAACAGA-3'
		Reverse	5'-CCAACTTTTGGCATAAGGTACTG-3'

Fluorescence photography

Fluorescence images were photographed using the Leica DC500 CCD Digital Camera mounted on the Leica M165FC fluorescence microscope (Leica Microsystem, Wetzlar, Germany). The mCherry filter (Leica

Microsystem) was used to screen the DR-GFP line. The GFP3 filter (Leica Microsystem) was used to observed repaired *SceGFP* after the HDR.

Total RNA extraction

Injected and uninjected embryos were collected at 48 h post-injection. Injected embryos were sorted based on the presence of eGFP expression and its total RNA was extracted in the presence of Sepasol-RNA I solution (Nacalai Tesque) according to the manufacturer's protocol. The total RNA was purified using phenol/chloroform extraction, precipitated with 70% ethanol, dissolved in UltraPure water (Invitrogen), and directly subjected to reverse transcriptase reaction.

Quantitative reverse-transcription PCR (qPCR)

cDNAs were synthesized from 1 μg of purified total RNA using random primers and PrimeScript II 1st strand cDNA Synthesis Kit (TaKaRa). The *β-actin* gene was amplified by PCR to confirm the absence of genomic DNA contamination as previously described[36]. To quantify repaired *SceGFP* mRNA level, qPCR was performed in StepOnePlus (Applied Biosystem) using KOD SYBR® qPCR Mix (Toyobo, Osaka, Japan) with primers as listed in Table 2. The cycling condition is as follows: 2 mins at 98^{o}C, followed by a total of 40 cycles of 98^{o}C for 10 s, 60^{o}C for 10 s, and 68^{o}C for 30 s. Primers' specificity was confirmed by melting curve analysis and agarose gel electrophoresis. The expression level of *eGFP* was normalized using that of *mCherry* that is controlled under the same promoter.

Results

Customization of a DR-GFP reporter

To visualize the HDR by fluorescence in *D. magna*, a previously established DR-GFP reporter plasmid[20] was customized (Fig. 1A, B). A red fluorescent protein gene *mCherry* ORF was fused upstream of the *SceGFP* via a sequence encoding *Thosea asigna* virus 2A (T2A), which can lead to bicistronic expression of both mCherry and mutated/repaired eGFP proteins[37]. To distinguish the eGFP-expressing cells individually, the nuclear localization signal was included in the *SceGFP*. At 6 bp upstream of the I-SceI recognition site, we also introduced a recognition site (5' -TCGA- 3') of a four-base endonuclease TaqI to allow us for visualizing HDR not only by the targeted DSB with I-SceI but also by the multiple DSBs with TaqI on the genome[38]. DR-GFP reporter will function when the DSB is introduced in the I-SceI site by the Cas9-gRNA complex. By SDSA or non-crossover DSBR subpathway of HDR, *SceGFP* will use *iGFP* as a repair template resulting in the functional eGFP expression (Fig. 1C). To express the DR-GFP reporter, we chose a 2.3 kb of *D. magna EF1α-1* genomic fragment including the promoter/enhancer, the transcription start site, the complete first intron, and part of the second exon with a start codon[39]. In addition, to recapitulate *EF1α-1* endogenous expression, the full-length *EF1α-1* 3' UTR was added downstream of the reporter. The complete nucleotide sequence of the customized DR-GFP reporter and the deduced amino sequence is provided in Supplementary Figure S1.

Generation of HDR reporter transgenic Daphnia

To integrate the customized DR-GFP reporter into *D. magna* genome, the CRISPR/Cas-mediated knock-in via non-homologous end-joining was used[29]. As a target site for knock-in of the reporter plasmid, we chose exon 3 of the eye pigment transporter *scarlet* gene[33]. We co-injected 50 ng/μL reporter plasmid and the RNP complex into 29 eggs. The 10 injected embryos survived until adult, from which 9 produced offspring with a white eye that is the typical phenotype of the *scarlet* mutant, indicating that the Cas9 RNP induced DSBs at the targeted site. Of the 9, one adult produced offspring with ubiquitous mCherry fluorescence, suggesting germline transmission of reporter plasmid (Fig. 2A). This fluorescence pattern also indicates that this reporter system enables us to detect the HDR event in most type of cells. We cultured this potentially transgenic line for genotyping.

To investigate whether NHEJ-mediated knock-in occurred, genotyping was performed using the genome of the potentially transgenic line. We amplified the mCherry fragment, 5' and 3' junctions between the transgene and its surrounding region by PCR (Fig. 2B). The expected size of the mCherry fragments was obtained only in the potential transgenic line (Fig. 2C, fragment B, DR-GFP line). The 3' junction region was also amplified in this line by using forward primer targeted at the downstream of *EF1α-1* 3' UTR of the donor plasmid and reverse primer targeted exon 8 of *scarlet* gene locus (Fig. 2B; Fig. 2C, fragment C, DR-GFP line). Sequencing of this PCR product confirmed the integration of the reporter plasmid at the *scarlet* locus and revealed 20 bp deletion and 8 bp insertion at the 3' side of the integrated cassette (Fig. 2D, 3´ junction). Consistent with the white-eyed phenotype, another allele contained indel mutation at the DSB site (Fig. 2D, 2nd allele). We were unable to amplify the 5' junction region even if the forward primer was designed at 3,157 bp upstream and 2,610 bp downstream of the DSB site. This suggests that large deletion occurred at the 5' side of the integration site. Nevertheless, amplification and sequencing of the full-length of the DR-GFP gene cassette demonstrated the integration of the intact DR-GFP reporter (Supplementary Figure S1). We then named this knock-in daphniid the DR-GFP line.

The DSB near the I-SceI site leads to the generation of eGFP-positive cells in embryos of the DR-GFP line

To determine whether DSBs induce HDR within the DR-GFP reporter system, we attempted to introduce DSBs with Cas9 and gRNA named SceI gRNA that target the *SceGFP*. The DSB by this Cas9 RNP occurs 2 bp upstream of the I-SceI recognition site that was previously used for I-SceI-dependent DSBs[20]. To confirm whether Cas9 is active during microinjection, we planned to co-inject the SceI gRNA with another gRNA targeting *Distal-less (Dll)* gene. This is because knockdown of *Dll* in embryos of *D. magna* led to a distinct phenotype “truncation of second antennae” and the level of this truncation corresponded to the degree of impairment of this gene[35]. The Dll gRNA was targeted to the upstream of the homeodomain region in exon 2 (Supplementary Figure S2), as this region is highly conserved among arthropod[35] and considered important for Dll function[40,41]. Injection of Cas9 and Dll gRNA into *D. magna* eggs resulted in 100% (13/13) truncation of second antennae (Supplementary Table S1). Of these, 8 (61.5%) showed the same strong phenotype as that induced by Dll RNAi[35]. This result suggests that Dll gRNA can be used as a marker for Cas9 activity during microinjection.

Seventy-four eggs were co-injected with 1 μM Cas9 protein and gRNA mixtures (SceI gRNA and Dll gRNA, 2 μM each). The phenotypes of the second antennae of the injected embryos were observed 48 hours post-injection (hpi). Forty-three embryos survived until the 48 hpi stage and 41 (95%) showed truncation of the second antennae (Table 3) from which, 22 embryos (54%) showed the strong phenotype[35], indicating that Cas9 was active during injection and could introduce DSBs on the genome. Of the 41, 33 (80%) showed strong nuclear-localized eGFP fluorescence in the tissues such as the head and thoracic appendages. (Fig. 3). In contrast, embryos injected with Cas9 RNP including the unrelated *St* gRNA (Fig. 3) and Dll gRNA did not show intense and nuclear-localized GFP signal, indicating that the recovery of the eGFP fluorescence occurred by injection of Cas9 protein and SceI gRNA.

Table 3
Summary of Cas9 protein, SceI gRNA, and Dll gRNA co-injection

Injected	Developed (48hpi)	Truncated antennae			Nuclear-localized eGFP
		Strong	Medium	Mild	
74	43	22/41 **(54%)**	9/41 **(22%)**	10/41 **(24%)**	33/41 **(80%)**

The embryos showing the nuclear-localized fluorescence signals have a functional eGFP gene repaired by HDR

To confirm whether HDR occurred at the genomic level, we extracted genome DNA from uninjected embryos and injected embryos that showed nuclear-localized eGFP fluorescence. PCR was then performed with a forward primer in the *mCherry* region and a reverse primer that recognizes specifically the sequence of the repaired *SceGFP* and (Fig. 4A, Fig. 4B). Because the reverse primer also can bind to the *iGFP* sequence that is a template for HDR (Fig. 4A), we expected two bands would appear upon genomic PCR. A higher size band (2,843 bp) was present in all samples, indicating amplification from iGFP sequence (Fig. 4C, ii), while a lower size band (1,048 bp) indicating amplification from repaired *SceGFP* sequence was obtained only from embryos injected with Cas9 and SceI gRNA (Fig. 4C, i). These results also suggest the repair of *SceGFP* by Cas9 and SceI gRNA.

We also attempted to develop a qPCR-based method that can detect the repaired SceGFP expression. We designed a forward primer that binds to the T2A-coding sequence of DR-GFP reporter locus, and a reverse primer that specifically binds to repaired *SceGFP* sequence (Fig. 5A). As a model to test this system, we used Cas9-mRNA and Cas9 protein for introducing the DSB on the *SceGFP* because mutagenesis efficiency with Cas9 mRNA was lower than that with Cas9 protein[29], which suggested Cas9 mRNA induces DSB occurrence to a lesser extent. We introduced the DSB at the *SceGFP* following either optimum condition of Cas9 mRNA (500 ng/μL Cas9 mRNA and 50 ng/μL gRNA) or Cas9 protein injection (1 μM Cas9 protein and 2 μM gRNA) [34,29]. The Dll gRNA was co-injected to evaluate the Cas9 activity in each injection. We confirmed 54% of Cas9 protein injected embryos showed a strong phenotype of

second antennae truncation while Cas9 mRNA could only introduce a mild phenotype (Table 3 and Table 4). This result implied that Cas9 protein had stronger activity to introduce DSB. Subsequently, the level of repaired *SceGFP* was analyzed using qPCR. By Cas9 protein injection, we observed significantly higher expression of repaired *SceGFP* (~ 5 fold) relative to Cas9 mRNA injection. Moreover, neither repaired *SceGFP* signal nor amplification was detected in uninjected embryos as well as scarlet gRNA injected embryos (Fig. 5B, Supplementary Fig. 3). Our result shows that qPCR can be used to detect the functional eGFP repaired by HDR.

Table 4
Summary of Cas9 mRNA, SceI gRNA, and Dll gRNA co-injection

Injected	Developed (48hpi)	Truncated antennae			Nuclear-localized eGFP
		Strong	Medium	Mild	
24	10	0	0	8/8 **(100%)**	**Not observed***

*To confirm the integrity of the Cas9 mRNA, the eGFP mRNA was also co-injected for confirmation of the mRNA integrity based on the eGFP fluorescence intensity. This prevented us from observing the nuclear-localized eGFP signals in the Cas9 mRNA-injected embryos.

Conclusion And Prospects

Here, we report a transgenic *D. magna* that can visualize HDR occurrence. The customized DR-GFP reporter plasmid was successfully introduced into the genome by NHEJ-mediated knock-in using CRISPR/Cas. DR-GFP reporter is known to respond to SDSA repair that occurs predominantly in mitotic cells[8]. We evaluated the functionality of this reporter system by introducing targeted DSB in the reporter site. We observed the eGFP signal and detected PCR products from the repaired eGFP gene in the injected daphniids, demonstrating evidence of detection of HDR *in situ* based on the eGFP fluorescence. We could also detect the repaired eGFP by qPCR that is potentially used for quantitative measurement of the HDR level following DNA DSB occurrences in the future. Furthermore, ubiquitous expression of mCherry that is bicistronically expressed with the DR-GFP suggests that this reporter system enables us to detect the HDR event in most types of cells.

We also acknowledge the limitations of this reporter system. First, in live imaging, it may be difficult to detect the eGFP signals from mutated cells that are located deep inside the tissues, which may lower sensitivity for detecting eGFP positive cells and their quantification. This limitation could be addressed by sorting and counting the eGFP-positive cells using fluorescence-activated cell sorting (FACS). Second, the DR-GFP reporter system can only visualize the presence of HDR events at the reporter locus. This situation may affect the sensitivity for detection of the HDR triggered by environmental genotoxicants or mutagenic agents that may introduce random DSB throughout the genome. Therefore, other approaches to globally visualize HDR events in *Daphnia* may be developed. For instance, fusing the Förster resonance energy transfer (FRET) system in HDR key proteins to provide spatiotemporal visualization of their

function[42]. Third, for a comprehensive understanding of the DNA repair mechanism in this species, reporters for detection of the other DNA repair pathways such as NHEJ and SSA need to be developed. This limitation can be addressed by utilizing other reporter systems, such as “traffic light”, a dual fluorescence-based reporter which can visualize HDR and NHEJ repair pathways[43].

Despite these possible limitations, DR-GFP reporter *Daphnia* would be a valuable tool to detect HDR in the context of live tissues and living animals. This approach eventually may contribute to molecular understanding toxicity of the genotoxicants to *D. magna*. The DR-GFP *Daphnia* would also achieve analyses and identification of components involved in HDR *in vivo*, which in turn contributes to the improvement of the HDR-based gene knock-in in this species. We also anticipate the prospect of utilizing this transgenic *Daphnia* for studying the function and roles of HDR in asexual reproduction.

Declarations

Author contributions

R.M.F., N.A., Y.K., and H.W. conceived and designed the study. R.M.F. made the transgenic animal, performed the main experiments, and wrote the original draft. R.M.F., N.A., and Y.K edited the manuscript. H.W. supervised the experiments and finalized the manuscript. All authors discussed the results, commented, and reviewed the manuscript.

Acknowledgments

pDRGFP plasmid was a gift from Maria Jasin (Addgene plasmid #26475). This work was supported by funding from the Japan Society for Promotion of Science (Grant Nos. 20H04923, 19H05423, 18H04884, 17H05602, 17K19236, and 17H01880). One of the authors (R.M.F) would like to acknowledge the Ministry of Education, Culture, Sports, Science and Technology (MEXT) for providing financial support under the Monbukagakusho/MEXT scholarship.

References

1. Aguilera, A. & Gómez-González, B. Genome instability: A mechanistic view of its causes and consequences. *Nat. Rev. Genet*, **9**, 204–217 (2008).
2. Huertas, P. DNA resection in eukaryotes: deciding how to fix the break. *Nat Struct Mol Biol*, **17**, 11–16 (2010).
3. Li, X. & Heyer, W. D. Homologous recombination in DNA repair and DNA damage tolerance. *Cell Res*, **18**, 99–113 (2008).
4. Szostak, J. W., Orr-Weaver, T. L., Rothstein, R. J. & Stahl, F. W. The double-strand-break repair model for recombination., **33**, 25–35 (1983).

5. Allers, T. & Lichten, M. Differential timing and control of noncrossover and crossover recombination during meiosis., **106**, 47–57 (2001).
6. Morrow, D. M., Connelly, C. & Hieter, P. 'Break copy' duplication: A model for chromosome fragment formation in Saccharomyces cerevisiae., **147**, 371–382 (1997).
7. Lin, F. L., Sperle, K. & Sternberg, N. Model for homologous recombination during transfer of DNA into mouse L cells: role for DNA ends in the recombination process. *Mol. Cell. Biol*, **4**, 1020–1034 (1984).
8. Andersen, S. L. & Sekelsky, J. Meiotic versus mitotic recombination: Two different routes for double-strand break repair. *BioEssays*, **32**, 1058–1066 (2010).
9. Yeh, C. D., Richardson, C. D. & Corn, J. E. Advances in genome editing through control of DNA repair pathways. *Nat. Cell Biol*, **21**, 1468–1478 (2019).
10. Chu, C. *et al.* Homologous recombination-mediated targeted integration in monkey embryos using TALE nucleases. *BMC Biotechnol*, **19**, 1–10 (2019).
11. Mao, Z., Bozzella, M., Seluanov, A. & Gorbunova, V. Comparison of nonhomologous end joining and homologous recombination in human cells. *Comp. nonhomologous end Join. Homol. Recomb. Hum. cells*, **7**, 1765–1771 (2008).
12. Mao, Z., Bozzella, M. & Seluanov, A. and V. G. DNA repair by nonhomologous end joining and homologous recombination during cell cycle in human cells. *Int. J. Biochem. Mol. Biol*, **1**, 1–11 (2010).
13. Puchta, H. The repair of double-strand breaks in plants: Mechanisms and consequences for genome evolution. *J. Exp. Bot*, **56**, 1–14 (2005).
14. Pardo, B., Gómez-González, B. & Aguilera, A. DNA double-strand break repair: How to fix a broken relationship. *Cell. Mol. Life Sci*, **66**, 1039–1056 (2009).
15. Chu, V. T. *et al.* Increasing the efficiency of homology-directed repair for CRISPR-Cas9-induced precise gene editing in mammalian cells. *Nat. Biotechnol*, **33**, 543–548 (2015).
16. Nakanishi, T., Kato, Y., Matsuura, T. & Watanabe, H. TALEN-mediated homologous recombination in Daphnia magna. *Sci. Rep*, **5**, 1–10 (2015).
17. Lin, S., Staahl, B. T., Alla, R. K. & Doudna, J. A. Enhanced homology-directed human genome engineering by controlled timing of CRISPR/Cas9 delivery. *Elife*, **3**, (2014). e04766
18. Charpentier, M. *et al.* CtIP fusion to Cas9 enhances transgene integration by homology-dependent repair. *Nat. Commun*, **9**, 1–11 (2018).
19. Słabicki, M. *et al.* A genome-scale DNA repair RNAi screen identifies SPG48 as a novel gene associated with hereditary spastic paraplegia. *PLoS Biol*, **8**, e1000408 (2010).
20. Pierce, A. J., Johnson, R. D., Thompson, L. H. & Jasin, M. XRCC3 promotes homology-directed repair of DNA damage in mammalian cells service XRCC3 promotes homology-directed repair of DNA damage in mammalian cells.*Genes Dev.*2633–2638(1999).
21. Paliwal, S., Kanagaraj, R., Sturzenegger, A., Burdova, K. & Janscak, P. Human RECQ5 helicase promotes repair of DNA double-strand breaks by synthesis-dependent strand annealing. *Nucleic*

Acids Res, **42**, 2380–2390 (2014).

22. Wang, R. *et al.* Double-strand break repair by homologous recombination in primary mouse somatic cells requires BRCA1 but not the ATM kinase. Proc. Natl. Acad. Sci. 110, 5564–5569(2013).
23. Johnson, N. M., Lemmens, B. B. L. G. & Tijsterman, M. A Role for the Malignant Brain Tumour (MBT) Domain Protein LIN-61 in DNA Double-Strand Break Repair by Homologous Recombination. *PLoS Genet*, **9**, e1003339 (2013).
24. Bekker, E. I. *et al.* Phylogeography of Daphnia magna Straus (Crustacea: Cladocera) in Northern Eurasia: Evidence for a deep longitudinal split between mitochondrial lineages. *PLoS One*, **13**, 1–20 (2018).
25. Herbert, P. D. N. The Population Biology of Daphnia (Crustacea, Daphnidae). Biol. Rev. 53, 387–426 53, 387–426(1978).
26. Tucker, A. E., Ackerman, M. S., Eads, B. D., Xu, S. & Lynch, M. Population-genomic insights into the evolutionary origin and fate of obligately asexual Daphnia pulex. Proc. Natl. Acad. Sci. U. S. A. 110, 15740–15745(2013).
27. Arao, T. *et al.* Production of genome-edited Daphnia for heavy metal detection by fluorescence. *Sci. Rep*, **10**, 1–10 (2020).
28. Törner, K., Nakanishi, T., Matsuura, T., Kato, Y. & Watanabe, H. Genomic integration and ligand-dependent activation of the human estrogen receptor α in the crustacean Daphnia magna. *PLoS One*, **13**, 1–11 (2018).
29. Kumagai, H., Nakanishi, T., Matsuura, T., Kato, Y. & Watanabe, H. CRISPR/Cas-mediated knock-in via nonhomologous end-joining in the crustacean Daphnia magna. *PLoS One*, **12**, 1–12 (2017).
30. Nakanishi, T., Kato, Y., Matsuura, T. & Watanabe, H. TALEN-mediated knock-in via non-homologous end joining in the crustacean *Daphnia magna*.*Nat. Publ. Gr.*1–7(2016).
31. Klüttgen, B., Dülmer, U., Engels, M. & Ratte, H. T. ADaM, an artificial freshwater for the culture of zooplankton. *Water Res*, **28**, 743–746 (1994).
32. Izzatur, N., Ismail, B., Kato, Y., Matsuura, T. & Id, H. W. Generation of white-eyed Daphnia magna mutants lacking scarlet function. *PLoS One*, **11**, 1–11 (2018).
33. Adhitama, N., Matsuura, T., Kato, Y. & Watanabe, H. Monitoring ecdysteroid activities using genetically encoded reporter gene in Daphnia magna. *Mar. Environ. Res*, **140**, 375–381 (2018).
34. Nakanishi, T., Kato, Y., Matsuura, T. & Watanabe, H. CRISPR/Cas-mediated targeted mutagenesis in *Daphnia magna*.*PLoS One***9**, (2014).
35. Kato, Y. *et al.* Development of an RNA interference method in the cladoceran crustacean Daphnia magna. *Dev. Genes Evol*, **220**, 337–345 (2011).
36. Kato, Y. *et al.* A 5' UTR-Overlapping LncRNA Activates the Male-Determining Gene doublesex1 in the Crustacean Daphnia magna. *Curr. Biol*, **28**, 1811–18174 (2018).
37. Kumagai, H., Matsuura, T., Kato, Y. & Watanabe, H. Development of a bicistronic expression system in the branchiopod crustacean Daphnia magna. *Genesis*, **55**, 1–6 (2017).

38. Muramoto, N. *et al.* Phenotypic diversification by enhanced genome restructuring after induction of multiple DNA double-strand breaks. *Nat. Commun*, **9**, 1–15 (2018).
39. Kato, Y., Matsuura, T. & Watanabe, H. Genomic Integration and Germline Transmission of Plasmid Injected into Crustacean Daphnia magna Eggs. *PLoS One*, **7**, 0–6 (2012).
40. Panganiban, G. & Rubenstein, J. L. R. Developmental functions of the Distal-less/Dlx homeobox genes. *Development*, **129**, 4371–4386 (2002).
41. McGinnis, W. & Krumlauf, R. Homeobox genes and axial patterning., **68**, 283–302 (1992).
42. Gibbs, D. R. & Dhakal, S. Homologous recombination under the single-molecule fluorescence microscope. *Int. J. Mol. Sci*, **20**, 1–16 (2019).
43. Certo, M. T. B. Y. *et al.* A. M. S. Tracking genome engineering outcome at individual DNA breakpoints. *Nat Methods*, **8**, 671–676 (2018).

Figures

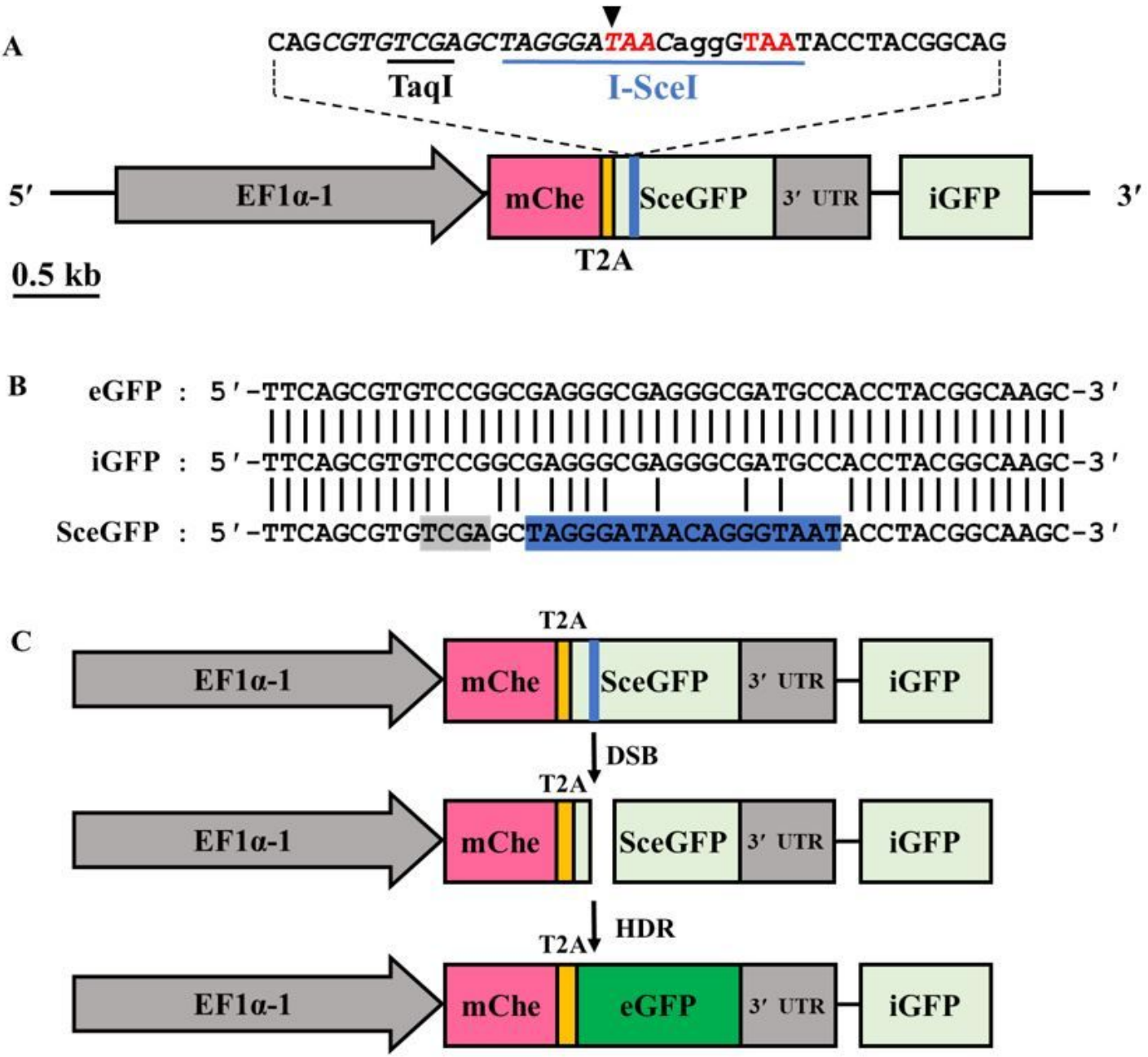

Figure 1

DR-GFP reporter system. (A) The donor plasmid design. The direct repeat of differentially mutated eGFP (DR-GFP) consists of mutated (SceGFP) and 5' and 3'-lacking sequence of eGFP (iGFP), both are indicated in light green boxes. Three repeats (two complete and one partial) of the simian virus 40 large T-antigen nuclear localization signal (SV40 NLS) are included in the SceGFP sequence (Supplementary Figure S1). The reporter system is expressed ubiquitously under D. magna EF1α-1 promoter/enhancer (grey arrow). The red fluorescence protein mCherry-coding sequence is placed upstream of the DR-GFP system. mCherry and DR-GFP are bicistronically expressed using Thosea asigna virus 2A (T2A) peptide indicated in the yellow box. SceGFP contains a recognition site of the 18 bp I-SceI restriction enzyme and

in-frame two stop codons indicated in the blue underline and red-letter respectively. SceI gRNA was designed to correspond with the I-SceI recognition site (italic) upstream of the PAM sequence (small letter). The cleavage site of SceI gRNA was indicated by a black triangle. The black underline indicates the TaqI recognition site. (B) The alignment between eGFP, iGFP, and SceGFP sequences. Blue and grey areas indicate the I-SceI and TaqI recognition sites respectively. (C) The diagram of the DR-GFP system for reporting HDR events. Double-strand break (DSB) is introduced in the I-SceI site by the Cas9-gRNA complex. Following homology-directed repair (HDR) occurrence, iGFP will serve as a repair template, leading to SceGFP repair indicated by eGFP expression green box.

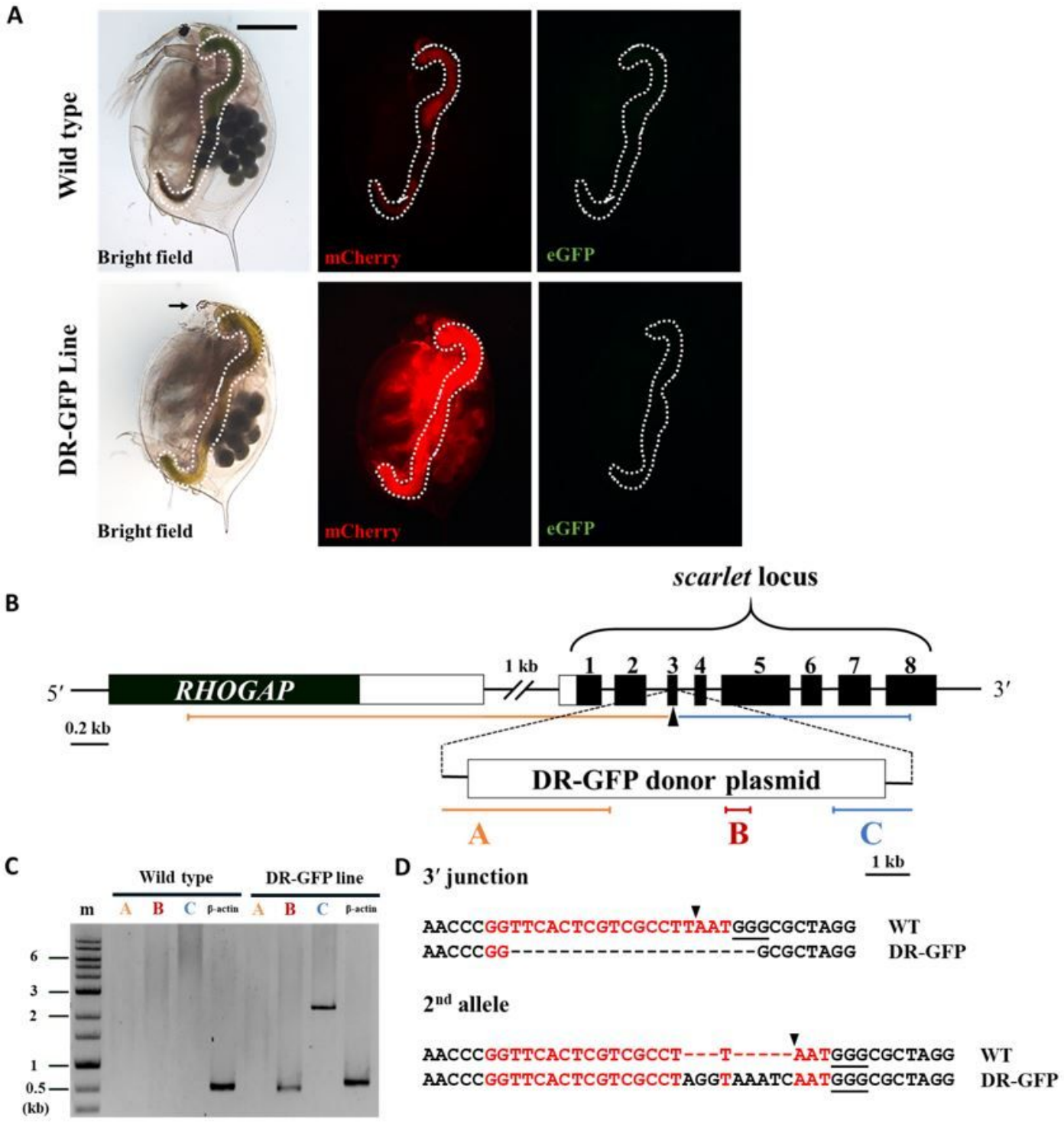

Figure 2

The phenotype and genotype of the DR-GFP line (A) Comparing phenotypes of the DR-GFP line with the wild type Daphnia. The top and lower rows show D. magna obtained from wild type and DR-GFP line respectively. The image in each column was photographed using either of bright field, mCherry, or GFP3 filter. The region inside the white-dashed line is the gut, in which ingested chlorella emits slight red autofluorescence both in wild type and DR-GFP. Widespread mCherry fluorescence was observed only in the transgenic line, while eGFP fluorescence was not observed. Black arrow indicates loss of black eye pigment due to disrupted scarlet allele. (B) Schematic representation of the integration site of the DR-GFP donor plasmid. A part of the RHOGAP (Rho-GTPase activating protein) gene is shown upstream of scarlet. The DR-GFP donor plasmid was integrated into exon 3 of the scarlet gene. A and C indicate the 5' and 3' junction regions of donor plasmid and genome, B indicated the internal region of donor plasmid (mCherry gene). (C) PCR result was visualized by gel electrophoresis. The first lane is the marker, followed by fragments A, B, C, and β-actin (beta-actin) for both wild type and DR-GFP line Daphnia. In the sample using DR-GFP line Daphnia, all fragments except the 5' junctions were amplified. The full length of the gel is presented in Supplementary Figure 4A. (D) 20 bp deletion and 8 bp insertion were detected in the 3' junction of plasmid integration and another allele of scarlet respectively. The red-colored nucleotides and black triangle indicated the St gRNA target and DSB site respectively.

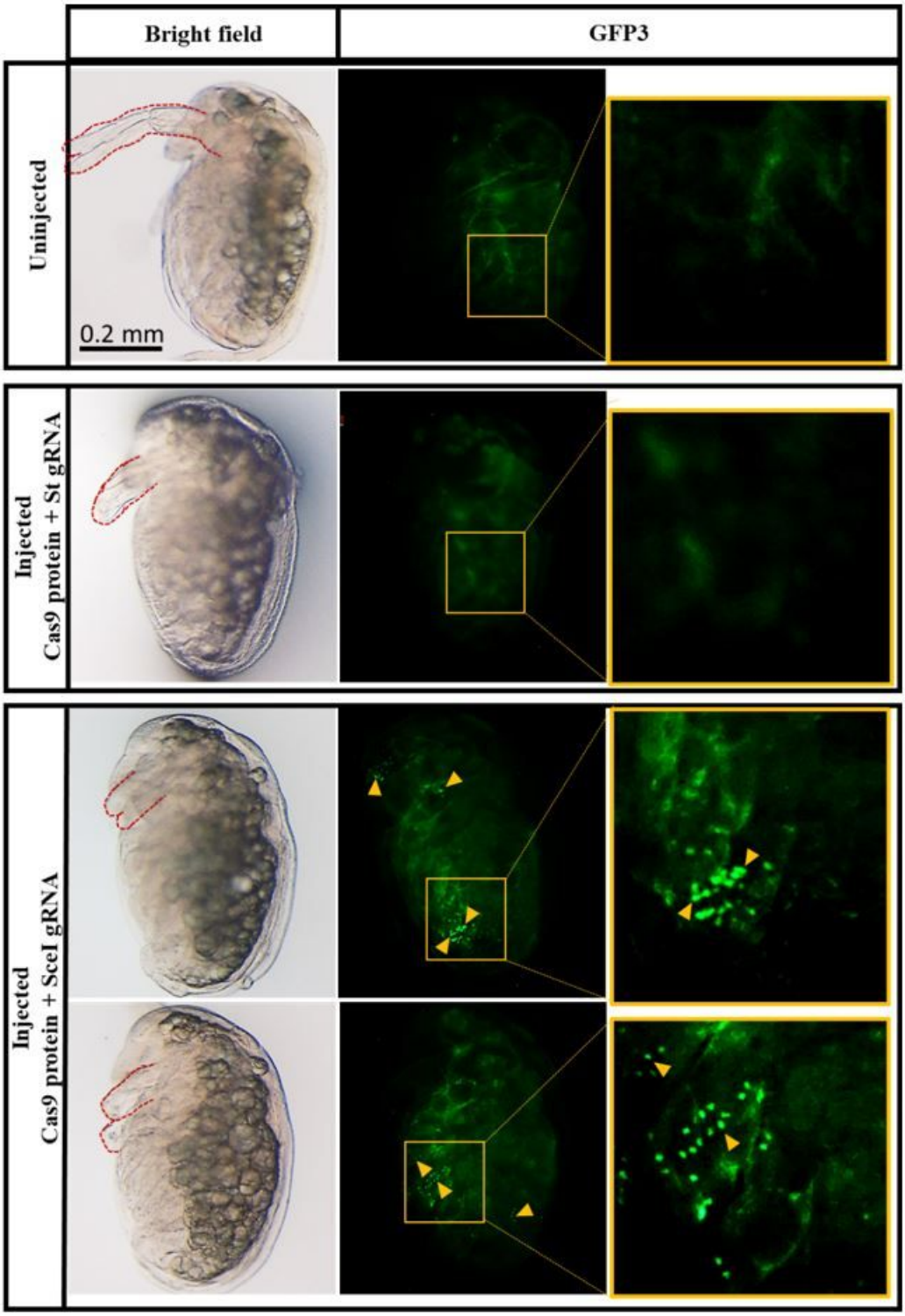

Figure 3

Detection of eGFP-positive cells of DR-GFP transgenic D. magna following the DSB of the SceGFP. DR-GFP line was co-injected with Cas9 protein, SceI gRNA, and Dll gRNA. The injection of Cas9 protein with St gRNA and Dll gRNA was performed as a control. The first row shows uninjected control, while the second, third, and fourth rows show injected individually Daphnia. Images were taken using the bright field and the GFP3 filter. All daphniids were photographed at 48 h post-injection. The red dashed line

shows the second antennae region, which was truncated because of Dll gRNA injection. The weak background green fluorescence observed throughout the body of all samples was coming from autofluorescence. The repaired SceGFP was controlled under EF1α-1 promoter/enhancer and contains NLS, resulted in abundantly expressed and nuclear-localized eGFP expression (yellow triangles).

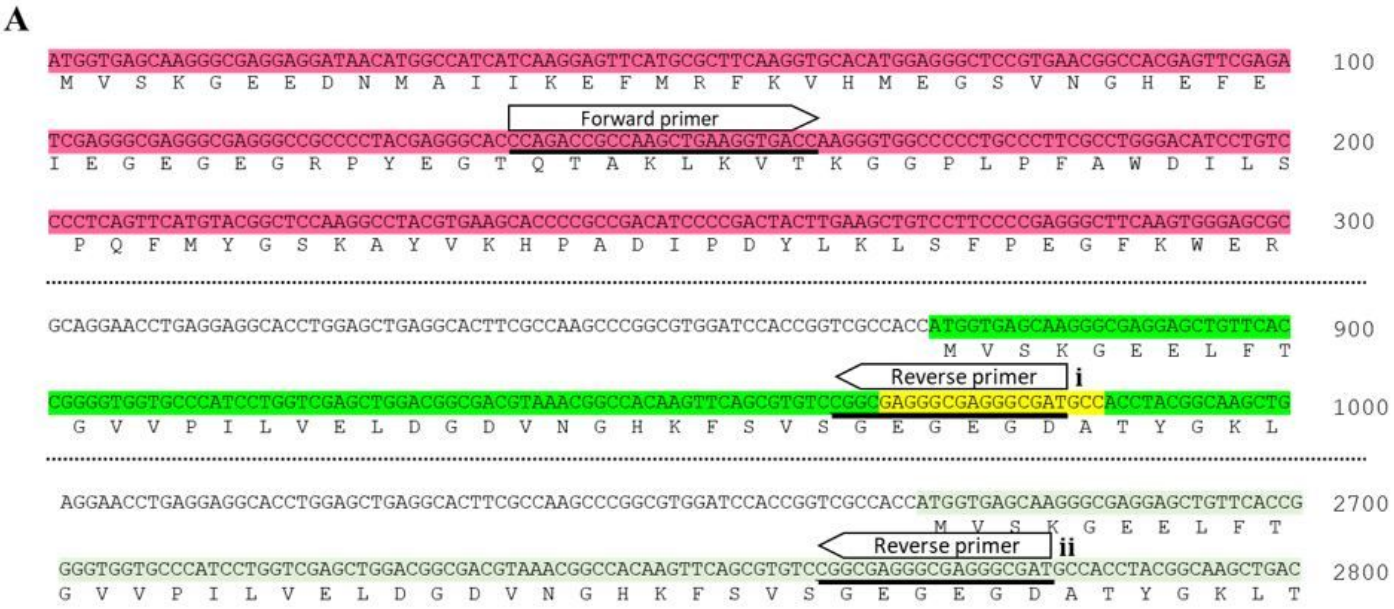

Figure 4

The genotype of DR-GFP transgenic after DSB introduction. (A) PCR was performed on uninjected and injected DR-GFP genome using primer pairs indicated by arrows. The forward primer is attached in the mCherry region (pink area) while the reverse primers are attached in two locations, the repaired SceGFP (yellow area) and iGFP (light green). (B) Alignment between SceGFP and repaired SceGFP or eGFP. The

reverse primer was designed to bind specifically to the repaired SceGFP (underline). (C) Gel electrophoresis result. The most left lane indicated the DNA marker (m) followed by amplified genome fragments (lanes 1-9) from Cas9 Protein and SceI gRNA injected embryos. Uninjected DR-GFP (lanes 10-12) was used as the negative control. The primer set amplified the repaired SceGFP region with the length 1,048 bp (i). The reverse primer was also attached to the iGFP region, which resulted in a 2,843 bp length PCR product (ii). The full length of the gel is presented in Supplementary Figure 4B.

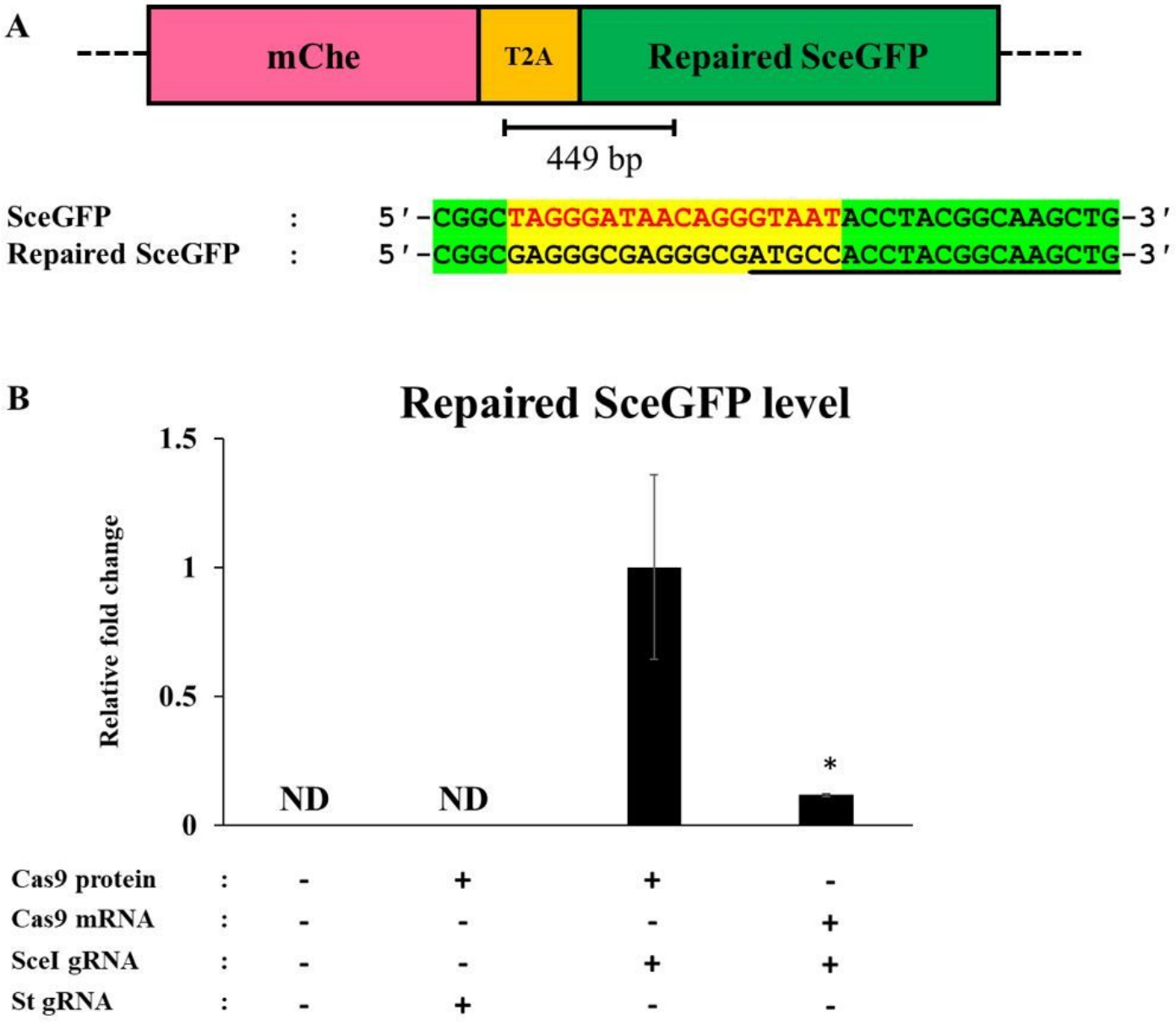

Figure 5

Detection of the functional eGFP transcript by qPCR. (A) The position of primers and the region used for quantifying the repaired SceGFP level (above) were shown in the black line. The alignment showed that the reverse primer was designed to specifically binds to repaired SceGFP fragment (underline). (B) Level

of repaired SceGFP between injected and uninjected samples after the introduction of DSB. The value was quantified by qPCR. There was a significant difference between Cas9 protein and mRNA injection. The values are means and error bars represent standard error (N=3). * $p<0.05$ (Student's t-test). In uninjected embryos and ones injected with Cas9 protein and scarlet gRNA, the repaired SceGFP mRNA was not detected (ND).

Supplementary Files

This is a list of supplementary files associated with this preprint. Click to download.

- Supplementaryinformationfinal2f.pdf